Supplementary information for the manuscript

Assignment of dynamic regions in biological solids enabled by spin-state selective NMR experiments

Rasmus Linser, Uwe Fink, and Bernd Reif*

Sample Preparation

A ^{2}H,^{13}C,^{15}N labelled sample of the SH3 domain of chicken α-spectrin was produced by recombinant protein expression. The protein was purified and micro-crystallized as described previously.[1] Protons were partially back-exchanged at labile positions by precipitating the protein in a buffer containing 25 % H_2O. This proton concentration was found to be the ideal compromise between sensitivity and resolution.[2] Spectra shown in Figures 1 G and H were recorded using a sample with a concentration of exchangeable protons of 10 %. Micro-crystals were obtained via a pH-shift from 3.5 to 7.5 overnight. The crystals were spun into a 3.2 mm rotor using approximately 15 mg protein per sample. We employed Paramagnetic Relaxation Enhancement (PRE) for accelerated data acquisition (150 mM and 75 mM Cu(edta) in the crystallization buffer for the sample containing 10 % and 25 % H_2O, respectively).[3]

NMR Experimental Details

NMR experiments shown in Figures 1 and 3 of the main manuscript were carried out on a Bruker Biospin AVANCE spectrometer operating at a ^{1}H Larmor frequency of 700 MHz. Experiments represented in Figure 2 of the main manuscript were performed on a 600 MHz spectrometer. In all experiments a 3.2 mm triple-resonance probe was employed, adjusting the MAS frequency to 24 kHz. H/N-correlations and triple-resonance-experiments were recorded with t_1^{max} = 80 and 22 ms, respectively. The effective temperature was set to ~ 22 °C if not denoted otherwise. This temperature takes heating effects due to sample rotation into account.[3] Data procession was performed using Bruker Topspin and Sparky.[4] Apodization in the indirect dimensions was achieved by application of gaussian multiplication using a line broadening of -10 Hz and a shift of the bell by 0.1.

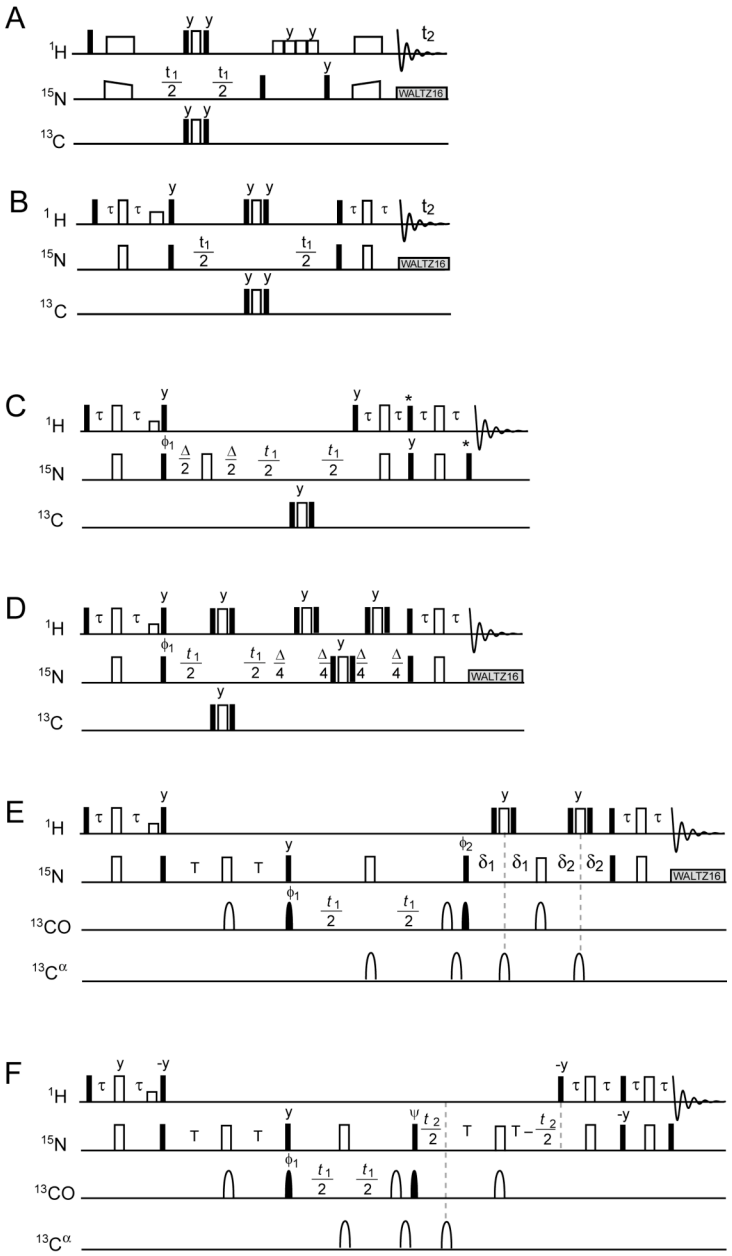

Figure S1: Pulse schemes. A) and **B)** H/N-correlations based on CP and INEPT magnetization transfer, respectively, used for Figure 1 in the main manuscript and Figure S1. Open and closed bars refer to 180° and 90° pulses, respectively. Water suppression was performed using four successive 15 ms/10 kHz purge pulses[5] in A) and a 1 ms purge pulse at 55 kHz in B) (pulses with reduced height). **C)** R_2 measurement. Using a ST2-PT building block,[6] $N^-H^{\alpha/\beta}$ coherences are transferred into observable H^- magnetization without mixing of spin-states. For spin state discrimination, a 2-step phase cycle (x, y) was applied to the first ^{15}N 90° pulse, requiring the receiver to follow in the opposite sense (x, -y). The scheme is adapted from Pervushin et al.[7,6] and is employed as well for the spin-state selective experiment yielding the spectrum shown in Supplementary Figure 5 (red contours). For swapping the selected coherence in the direct dimension from H^-N^α to H^-N^β, the phase of the ^{15}N pulse labelled with an asterisk is shifted by 180°. For swapping between N^-H^α and N^-H^β in the indirect dimension, the ^1H pulse labelled with an asterisk must be inverted.[8] Δ was set to 8 µs, 1 ms, 2 ms, 5 ms, 15 ms, 40 ms, 70 ms, respectively. **D)** Pulse scheme employed for the

H/N-correlation without spin-state selection (black) in Supplementary Figure 5. The delays Δ mimics the delay required for the evolution of $^1J_{N,C}$ scalar couplings during which relaxation can occur. **E)**, **F)** HNCO and HNCO-TROSY pulse schemes used for the experiment represented in Figure 3 of the main manuscript, adapted from Grziesek et al.[9], and Yang and Kay.[10] Open and closed bars represent 180° and 90° pulses, respectively. The open pulse with reduced height represents a 1 ms purge pulse for water suppression. τ and T were set to 2.17 and 12 ms, respectively. δ_1 and δ_2 represent the delays T/2-t_2/4 and T/2+t_2/4, respectively. For phase sensitivity in the indirect dimension, φ_1 and φ_2 were incremented according to TPPI. For phase sensitivity in the indirect ^{15}N dimension in the TROSY experiment, ψ was incremented in a clockwise/anticlockwise sense in steps of 90° in subsequent FIDs with the receiver following in the same/opposite sense using echo/antiecho detection. Selective ^{13}C pulses were applied using soft rectangular pulses on-resonance, and G3 shaped pulses[11] off-resonance. Exchange of pulses on the ^{13}CO and the $^{13}C^{\alpha}$ channel generates the HNCA experiment. Waltz-16 was used (ω_{rf} = 2 kHz) for heteronuclear scalar decoupling.

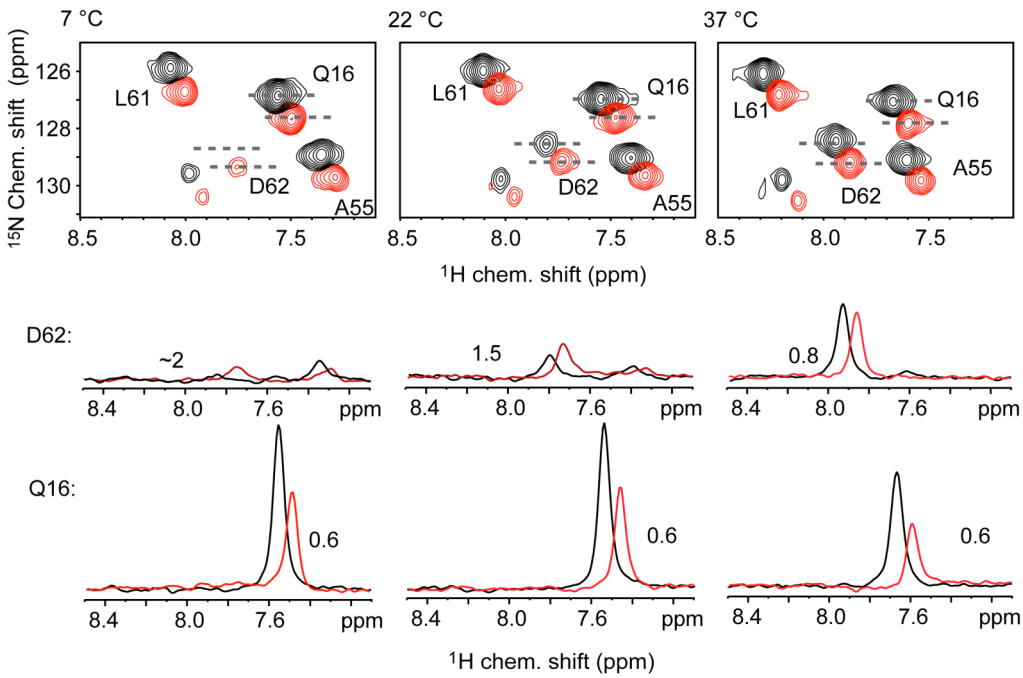

Figure S2: H/N correlation recorded with a ^{15}N-T_2 filter. The T_2 filter time was set to 48 ms, which corresponds to the typical scalar coupling evolution period in triple-resonance HNCO type experiments. Correlations which involve mixing of spin-states are depicted in black. Correlations recorded using spin-state selection are shown in red (see Supplementary Figure 3A and B for pulse schemes). For quantitative comparison, 1D cross-sections along the proton dimension (as indicated in the 2D by dashed lines) are represented at the bottom of the figure (for Q16, D62). Depending on the temperature, spin-state selection results in better sensitivity for mobile residues like D62. The factors indicated in the figures reflect the ratio of intensities between spin-state selective and standard experiment. The indicated temperatures refer to the effective temperatures in the sample, which are ~20 °C higher than the nominal temperatures due to MAS. TROSY peaks are shifted by $J_{NH}/2$ in both dimensions. Spectra were obtained using a deuterated sample which was prepared using 10 % H_2O in the crystallization buffer. The MAS frequency was set to 24 kHz at a ^{1}H Larmor frequency of 400 MHz.

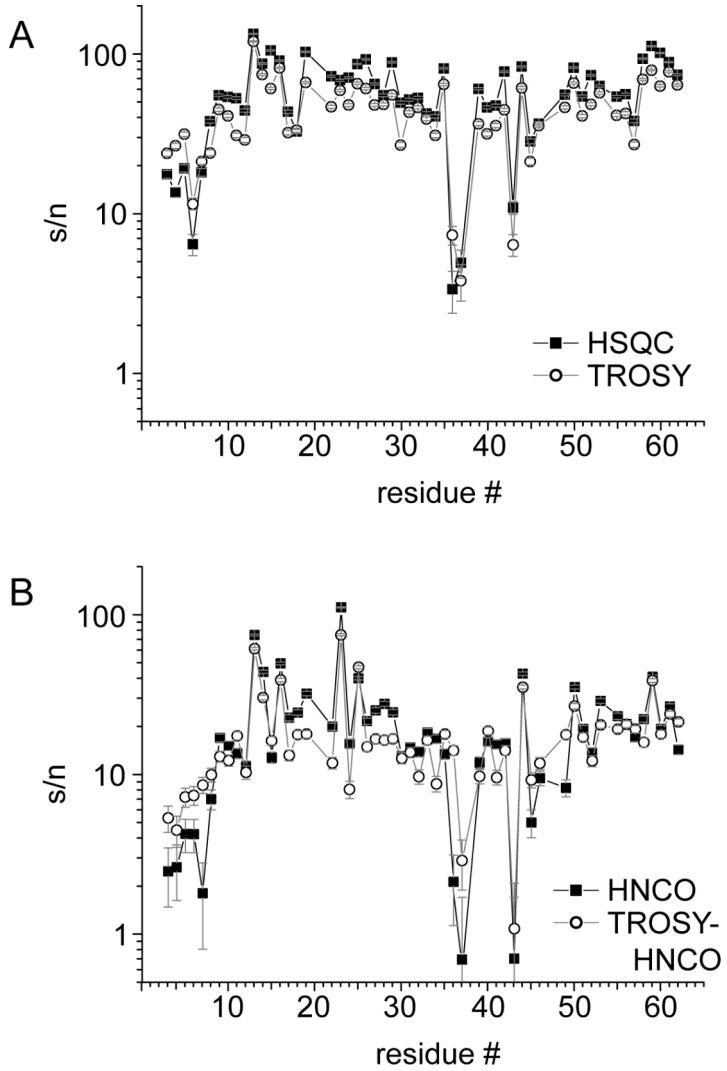

Figure S3: Comparison of relative intensities in an HSQC, TROSY, HNCO, and a TROSY-HNCO experiment. Although the overall performance of the spin-state selective experiments is worse due to scarification of part of the magnetisation and an increased number of pulses, mobile residues slightly gain in intensity using TROSY experiments in the double resonance experiments. The effect is severe, however, if triple-resonance experiments are considered. **A)** Residue specific signal-to-noise ratio of an HSQC (black squares) and a TROSY experiment (white circles). Both spectra were acquired recording 250 complex points (corresponding to a t_1^{max} = 65 ms), applying the same acquisition and processing parameters for both experiments. For apodization in the direct dimension, 5 Hz exponential line-broadening was applied. **B)** Residue specific signal-to-noise ratio of an HNCO (black squares) and a TROSY-HNCO (white circles). The experiments were recorded as 2Ds (H/N) without evolution of the ^{13}C dimension. Both experiments were recorded and processed using identical parameters (70 complex points in t_1, corresponding to t_1^{max} = 22 ms). In the direct dimension, the data were folded with an exponential function, applying line broadening of 30 Hz. In the indirect dimension, gaussian multiplication was used employing a line broadening of -10 Hz and a shift of 0.1. All spectra were recorded within 2 h on a 700 MHz spectrometer, adjusting the effective temperature to 22 °C and the MAS frequency to 24 kHz. The employed pulse schemes are depicted in Figure S3 E) and F).

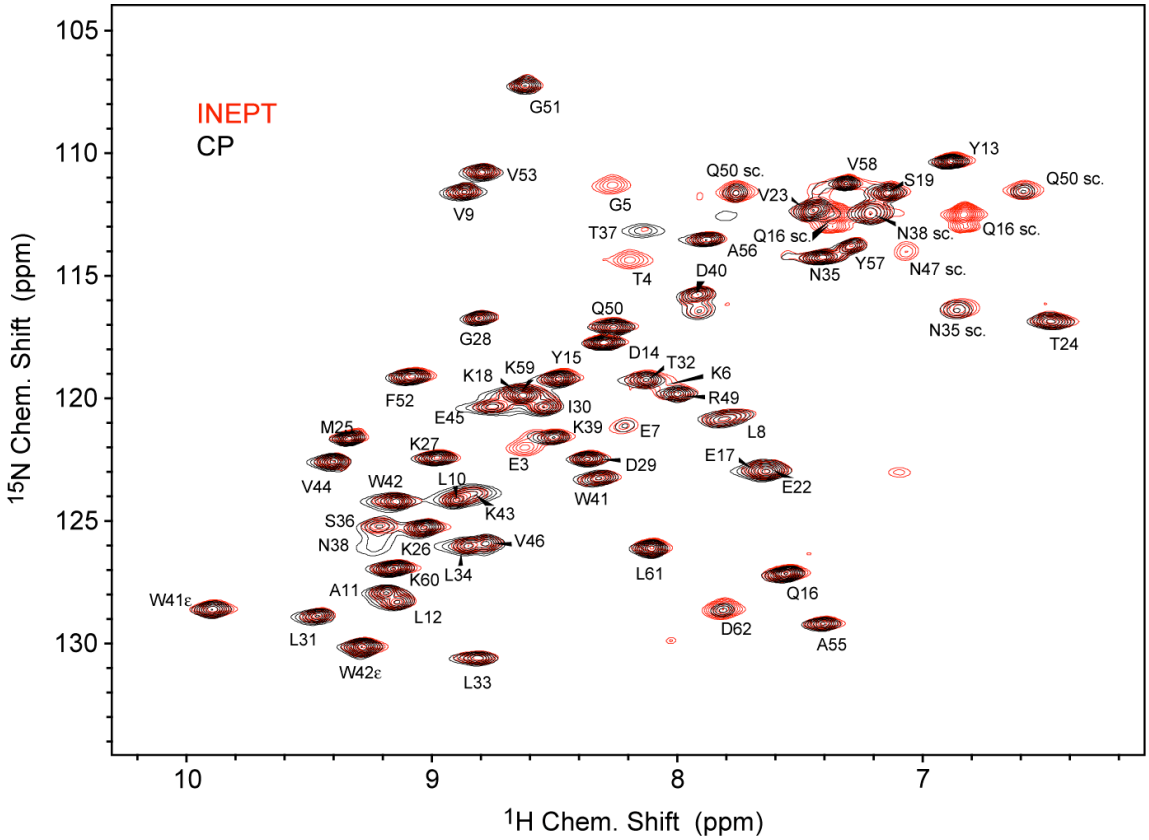

Figure S4. Complete H/N-correlation for the comparison of scalar (red) and dipolar transfer (black). The experiments were recorded at 600 MHz ^{1}H Larmor frequency at a temperature of 22 °C a MAS frequency of 24 kHz. Acquisition in the indirect dimension amounted to t_{1max} of 93 ms. In the direct dimension, the data were folded with an exponential function, applying line broadening of 10 Hz. In the indirect dimension, gaussian multiplication was used employing a line broadening of -10 Hz and a shift of 0.1. Both spectra were recorded within 2.5 h. The sample contained a proton content of 25 % at exchangeable sites and 75 mM Cu(edta) for PRE. The employed pulse schemes are depicted in Figure S3 A and B.

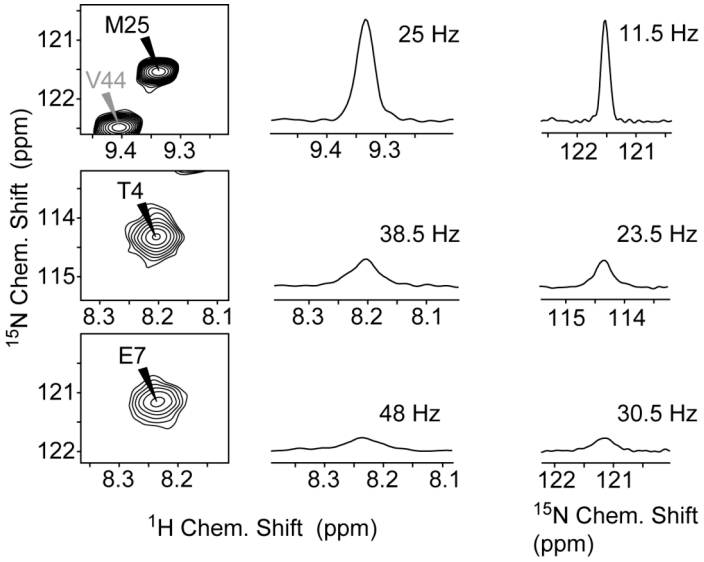

Figure S5. Line shapes extracted from a decoupled HSQC. For rigid residues, we find line widths on the order of 10-15 Hz and 10 Hz in the ^{1}H and ^{15}N dimension, respectively. For mobile residues, however, the line widths go up to 50 and 30 Hz, respectively, if no spin-state selection is employed. The H/N-correlation was recorded within 20 h for a sample crystallized from a solution containing 10 % H_2O and 150 mM Cu(edta). The MAS frequency was adjusted to 24 kHz and the effective temperature was set to 22 °C. 380 complex points were recorded in the indirect ^{15}N dimension, corresponding to t_1^{max} =100 ms. No apodization for procession was applied. Differences in line width are not due to PRE, as similar spectra are obtained using samples that are not doped with Cu(edta).

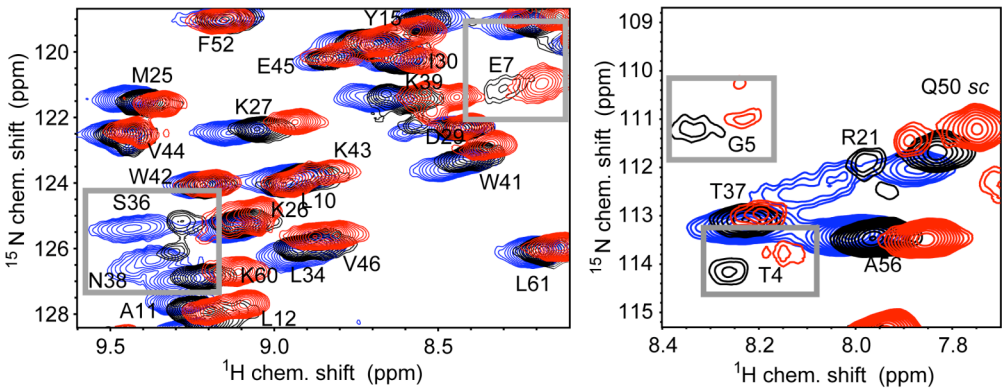

Figure S6: N/H correlations recorded for α-spectrin SH3 at different temperatures for a sample crystallized with a buffer containing 10 % H_2O. In order to optimize the sensitivity for resonances that could previously not be detected, we varied the temperature of the sample. We recorded non-spin state selective H/N-correlation experiments at set temperatures of –16 °C (blue), 2 °C (black), and 20 °C (red). The effective temperatures are 4 °C, 22 °C, and 42 °C due to sample rotation induced heating.[3] Resonances which yield higher intensities at either elevated or lower temperatures are highlighted by grey rectangles. The employed pulse scheme is depicted in Figure S3 B).The best signal to noise ratio for the problematic residues is obtained at moderate temperatures. All spectra were recorded, processed and plotted using identical parameters.

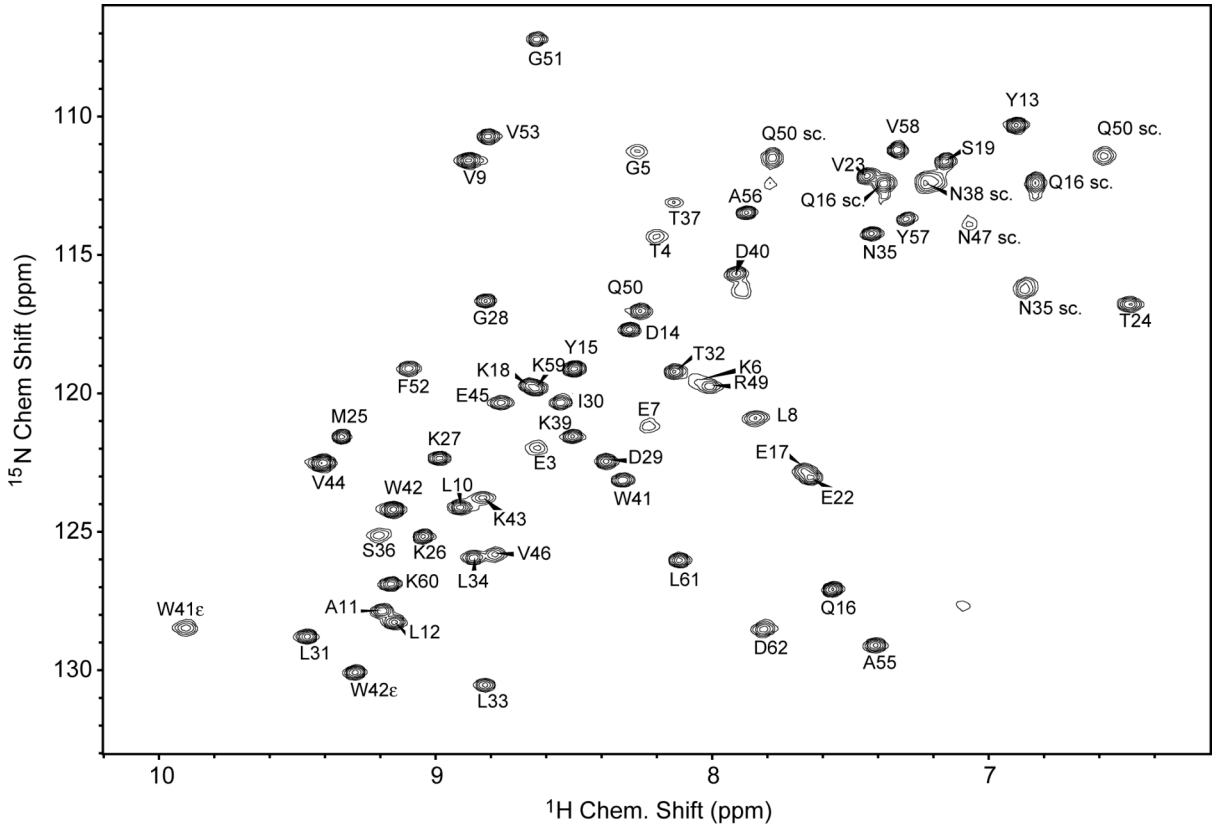

Figure S7. Assignment of the H/N-correlation of the α-spectrin SH3 domain. The spectrum was recorded as an HSQC for a deuterated sample with a concentration of 10 % protons in exchangeable sites, adjusting the effective temperature to 22 °C and the MAS frequency to 24 kHz MAS. Increments in the indirect dimension were acquired up to t_1^{max} = 80 ms. The data was processed using gaussian multiplication with line broadening of -10 Hz and a shift of the bell by 0.1 in the indirect ^{15}N dimension. For the direct ^{1}H dimension, a line broadening of 5 Hz for exponential multiplication was applied.

Residue	*INEPT*	*CP*
E3	66.3	6.5
T4	69.0	2.0
G5	69.2	3.7
K6	37.3	19.7
E7	38.9	34.5
L8	81.6	107.1
V9	147.8	177.4
L10	173.6	189.1
A11	153.9	171.9
L12	152.3	132.6
Y13	398.7	341.8
D14	358.3	265.9
Y15	297.7	249.7
Q16	395.0	286.1
E17	122.9	170.7
K18	85.3	97.6
S19	253.9	205.5
E22	212.4	195.4
V23	249.6	213.6
T24	149.2	141.0
M25	320.0	257.5
K26	292.4	242.5
K27	236.0	199.2
G28	177.3	167.3
D29	241.1	182.9
I30	137.9	163.5
L31	149.5	167.6
T32	161.5	134.0
L33	123.9	121.2
L34	128.7	144.7
N35	268.3	206.9
S36	66.4	76.5
T37	22.2	51.0

Residue	*INEPT*	*CP*
N38	10.8	36.5
K39	164.7	125.8
D40	128.7	119.1
W41	145.5	132.1
W42	215.7	201.3
K43	57.2	103.0
V44	221.7	228.9
E45	90.3	114.6
V46	96.6	139.8
R49	129.1	145.3
Q50	233.0	245.6
G51	159.5	161.6
F52	234.0	205.1
V53	195.2	199.1
A55	185.7	133.4
A56	210.9	163.5
Y57	132.2	122.5
V58	313.2	230.5
K59	350.0	332.4
K60	381.0	290.5
L61	292.5	264.5
D62	168.4	63.2
$Q16_{sc}$ (E)	472.0	33.4
$Q16_{sc}$ (Z)	456.2	17.5
$N35_{sc}$ (E)	39.3	57.5
$N35_{sc}$ (Z)	68.7	58.4
$N38_{sc}$ (Z)	131.8	123.8
W41 Nε1	211.0	162.2
W42 Nε1	305.1	272.9
$N47_{sc}$ (E)	24.7	29.7
$N47_{sc}$ (Z)	44.8	10.9
$Q50_{sc}$ (E)	192.1	82.4
$Q50_{sc}$ (Z)	91.8	58.8

Table 1. Signal to noise ratio of H/N-correlations recorded with INEPT and CP magnetization transfer. The values are plotted as a function of amino acid sequence in Figure 2B in the main manuscript. The peak intensities were extracted from the spectra shown in Supplementary Figure S1, see there for experimental details. The subscript sc refers to side chain amides.

	22 °C				3 °C			
Residue	$R_2(N^-H^\alpha)$	Δ	$R_2(N^-H^\beta)$	Δ	$R_2(N^-H^\alpha)$	Δ	$R_2(N^-H^\beta)$	Δ
E3	48.5	3.1	75.4	14.2	47.0	30.3	-	-
T4	48.6	2.5	111.9	16.1	-	-	-	-
G5	50.1	3.7	109.4	15.4	-	-	-	-
E7	41.6	3.8	124.4	48.0	-	-	-	-
L8	35.7	3.8	50.5	2.5	39.8	3.6	117.6	24.1
V9	33.7	4.4	41.4	4.9	31.1	3.6	38.0	4.4
L10	32.3	4.0	35.9	4.6	32.6	4.8	32.1	3.8
A11	30.5	4.7	34.6	8.8	33.5	4.5	25.5	8.7
L12	28.3	4.8	36.1	6.3	27.1	4.1	25.2	3.4
Y13	26.8	5.0	33.5	4.4	26.7	5.2	28.1	3.9
D14	27.5	4.6	31.5	4.6	21.1	3.6	24.5	3.1
Y15	33.0	4.1	33.4	4.5	23.9	3.6	22.9	3.3
Q16	29.4	4.2	33.5	4.8	26.1	2.3	28.7	3.3
E17	34.3	3.6	43.2	5.3	31.2	6.1	29.2	4.6
K18	54.6	10.9	32.0	7.8	21.7	5.4	27.6	3.4
S19	32.5	4.0	35.6	3.3	26.6	2.2	31.1	3.1
E22	34.1	3.6	34.4	3.7	48.3	37.0	27.5	3.2
V23	32.0	5.0	36.2	4.0	29.9	15.3	33.2	7.6
T24	36.5	3.5	37.7	3.2	27.5	2.5	31.7	3.1
M25	29.7	4.4	35.9	6.6	22.6	3.3	25.3	3.3
K26	29.2	4.3	31.0	3.9	25.1	3.0	27.4	8.9
K27	32.5	3.6	30.2	4.8	25.7	2.6	24.9	4.3
G28	31.2	4.3	30.7	4.1	26.4	4.5	20.9	4.4
D29	32.9	3.7	29.5	4.3	33.4	3.3	24.3	6.3
I30	34.4	4.1	33.2	5.3	28.2	3.4	32.2	3.4
L31	29.7	5.6	37.4	4.4	27.6	4.1	31.4	2.7
T32	33.0	4.5	44.8	3.3	28.4	2.9	38.3	6.2
L33	32.6	4.2	44.9	4.5	28.6	4.6	36.2	5.5
L34	34.2	3.9	38.3	3.2	31.5	3.8	28.3	6.3
N35	28.8	4.4	28.6	4.2	24.7	3.3	27.0	6.8
S36	118.1	28.4	32.4	29.5	32.3	0.9	50.9	12.0
T37	53.8	22.6	45.9	15.5	32.4	4.5	45.1	13.0
N38	-	-	-	-	53.3	12.0	59.3	13.0
K39	32.4	4.1	32.9	4.0	28.3	4.1	27.4	4.5
D40	30.3	4.4	34.2	3.5	29.4	3.8	34.9	4.3
W41	33.0	4.3	34.1	4.0	25.1	3.1	27.2	4.8
W42	35.2	3.2	37.4	4.3	31.2	3.7	29.6	3.0
K43	48.1	7.6	40.5	13.0	54.3	23.3	55.3	7.4
V44	34.4	3.8	36.2	5.5	26.3	2.2	26.2	2.5
E45	43.1	5.5	43.0	3.9	28.3	1.5	56.3	10.0
V46	32.5	4.1	43.2	2.8	31.6	3.9	65.6	14.0
R49	34.5	3.8	50.8	2.4	30.2	2.4	49.8	10.3
Q50	32.6	4.5	35.7	3.2	24.6	3.2	45.4	8.0
G51	37.4	3.1	46.6	13.7	33.1	4.0	28.4	2.3
F52	33.1	4.0	36.1	3.9	28.3	3.5	31.0	3.9
V53	32.7	3.8	36.2	3.6	31.7	3.2	37.8	4.4
A55	32.2	4.4	28.8	4.5	26.6	7.0	22.2	8.8
A56	29.0	4.5	36.0	5.2	21.6	4.0	25.1	3.6

Y57	32.8	7.8	34.3	8.7	20.3	4.3	16.8	8.2
V58	29.1	4.8	32.1	4.8	28.8	2.8	25.3	3.1
K59	31.9	3.8	36.2	4.5	24.2	3.2	27.3	3.3
K60	30.2	4.1	31.6	4.3	25.7	3.1	25.5	2.5
L61	29.7	4.2	33.5	4.7	26.9	2.5	34.6	5.6
D62	31.1	4.0	56.8	3.7	28.4	2.8	138.3	31.6
$Q16_{sc}$ (E)	32.9	5.0	33.7	4.2	30.1	1.5	37.8	3.1
$Q16_{sc}$ (Z)	30.2	4.2	29.9	3.9	36.1	4.2	33.6	3.8
$N35_{sc}$ (E)	103.4	85.3	59.7	10.9	-	-	1.7	13.6
$N35_{sc}$ (Z)	40.2	5.3	48.2	10.3	32.6	2.8	35.6	6.6
$N38_{sc}$ (Z)	32.0	3.5	33.4	4.3	35.6	4.2	28.0	3.2
W41 Nε1	37.5	3.0	54.9	1.8	25.1	3.9	28.3	2.3
W42 Nε1	33.4	3.9	31.7	4.3	29.4	2.8	27.1	3.7
$N47_{sc}$ (E)	62.3	4.3	99.2	13.7	-	-	71.1	31.2
$N47_{sc}$ (Z)	57.4	3.8	85.1	13.3	25.5	13.3	-	-
$Q50_{sc}$ (E)	34.2	4.4	34.8	4.6	35.1	3.6	38.7	4.9
$Q50_{sc}$ (Z)	37.7	4.5	31.9	2.9	39.7	3.8	38.0	7.4

Table 2. ^{15}N Relaxation rates for spin states $N^{-}H^{\alpha}$ and $N^{-}H^{\beta}$. Values given in Hz. Dashes refer to resonances for which no sensible fit could be obtained due to insufficient signal to noise. The subscript sc refers to side chain amides. The values, plotted as a function of amino acid sequence in Figure 3B in the main manuscript, were measured using the pulse sequence depicted in Supplementary Figure 1C. For the acquisition of raw data, 7 data sets with a delay Δ between 0 and 70 ms were recorded for each temperature and each spin state, employing 200 complex points (50 ms t_{1max}) in the indirect dimension. Each spectrum was recorded within 1 h. Data evaluation was performed with Sparky[4] and Origin[12] using fit functions of exponential decay. Δ denotes the error of this fit. Apodization was done by gaussian multiplication employing 10 Hz line broadening and a shift of the bell by 0.1 for the indirect dimension and 10 Hz exponential multiplication for the direct ^{1}H dimension. The employed sample contained 25 % ^{1}H in exchangeable sites and 75 mM Cu(edta). The spectra were recorded at 700 MHz ^{1}H Larmor frequency and 24 kHz MAS. Sample temperatures given in the first line take frictional heating by MAS into account.

References:

(1) Chevelkov, V., Faelber, K., Schrey, A., Rehbein, K., Diehl, A., Reif, B., *J. Am. Chem. Soc.* **2007**, *129*, 10195–10200.
(2) Akbey, Ü., Lange, S., Franks, W. T., Linser, R., Rehbein, K., Diehl, A., van Rossum, B.-J., Reif, B., Oschkinat, H., *J. Biomol. NMR* **2009**, *46*, 67-73.
(3) Linser, R., Chevelkov, V., Diehl, A., Reif, B., *J. Magn. Reson.* **2007**, *189*, 209–216.
(4) Goddard, T. D., Kneller, D. G., *SPARKY 3, University of California, San Francisco*.
(5) Zhou, D. H., Rienstra, C. M., *J. Magn. Reson.* **2008**, *192*, 167-172.
(6) Pervushin, K. V., Wider, G., Wüthrich, K., *J. Biomol. NMR* **1998**, *12*, 345-348.
(7) Pervushin, K. V., Riek, R., Wider, G., Wüthrich, K., *Proc. Natl. Acad. Sci. USA* **1997**, *94*, 12366-12371.
(8) Andersson, P., Annila, A., Otting, G., *J. Magn. Reson.* **1998**, *133*, 364-367.
(9) Grzesiek, S., Bax, A., *J. Magn. Reson.* **1992**, *96*, 432–440.
(10) Yang, D., Kay, L. E., *J. Biomol. NMR* **1999**, *13*, 3-10.
(11) Emsley, L., Bodenhausen, G., *Chem. Phys. Lett.* **1990**, *165*, 469-476.
(12) *Origin (Version 8), Northampton, MA: OriginLab Corporation.* **2007**.